

Ballistic Dark Matter oscillates above Λ CDM

Anirban Das, Basudeb Dasgupta, and Rishi Khatri

Tata Institute of Fundamental Research, Homi Bhabha Road, Mumbai, 400005, India.

E-mail: anirbandas@theory.tifr.res.in , bdasgupta@theory.tifr.res.in,
khatri@theory.tifr.res.in

Abstract. Dark matter may have been relativistic and collisional until relatively late times and become cold and collisionless after a phase transition before the matter-radiation equality of the standard Λ CDM cosmology. We show that such a dark matter has large peculiar velocities due to acoustic oscillations before the phase transition, and evolves ballistically after the phase transition in the collisionless phase until the initial acoustic velocities are redshifted away. We show that this Ballistic Dark Matter (BDM) results in new non-trivial interesting features in the cosmological observables. In particular, the linear matter power spectrum exhibits acoustic oscillations on scales smaller than the Hubble scale at the time of phase transition, and for fast transitions the power at the acoustic peaks in the matter power spectrum *exceeds* that in a Λ CDM cosmology. If BDM only forms a part of the total dark matter, an odd vs. even acoustic peak asymmetry becomes prominent. We give an approximate analytical treatment of the linear perturbations in BDM, explaining these features. We also discuss the possibility to constrain BDM using cosmic microwave background and large scale structure data.

Contents

1	Introduction	1
2	Ballistic Dark Matter: Model & Methods	3
3	Cosmological Signatures	4
3.1	Extra Relativistic Degrees of Freedom	4
3.2	Matter Power Spectrum	6
3.2.1	Analytical Understanding of the Acoustic Peaks	7
3.2.2	Odd-Even Peak Asymmetry	10
3.3	Qualitative Constraints from the Matter and CMB Power Spectrum	12
4	Summary & Conclusions	13

1 Introduction

Diverse lines of cosmological evidence suggest that approximately 84% of the total matter in the Universe behaves as if it were made of particles without appreciable interactions, either among themselves or with other particles, and with very small velocity dispersion, i.e., collisionless cold dark matter (CDM) [1–7]. In most particle physics models of dark matter, the dark component could not have been CDM-like at arbitrarily high redshifts. At early enough times, the dark component in most dark matter models would have been relativistic and collisional, coupled to itself and perhaps also with the visible sector. The dark component would become non-relativistic at some epoch and also (almost) collisionless, as the different interaction rates become slower than the expansion rate of the Universe, leading to chemical freeze-out and kinetic decoupling. These three transitions, viz., becoming non-relativistic, freeze-out of interactions with itself, and freeze-out with the visible sector, may or may not always coincide (See Ref. [8] for an example).

In the standard WIMP (weakly interacting massive particle) models, freeze-out of dark matter self-annihilations into visible sector particles, which fixes the dark matter abundance, happens long after the dark component is already non-relativistic. See Ref. [9] for an overview. On the other hand, in pure dark gauge sector models, dark gluons decouple from the visible sector very early and undergo a phase transition to form nonrelativistic dark glueballs, whose self-interactions may or may not be important [10–14]. Similarly, in asymmetric dark matter models with light dark quarks, the dark relativistic plasma condenses into nonrelativistic dark baryons which act as the dark matter [15–21]. We will club these theories, where a self-collisional dark radiation transitions to collisionless dark matter at some late redshift z_* , long after decoupling from the visible sector, under the rubric of “Ballistic Dark Matter” (BDM). Here *ballistic* refers to the fact that the dark matter at the beginning of the non-relativistic collisionless phase has large initial velocities inherited from the acoustic oscillations in the relativistic collisional phase.

In the BDM model, the time and duration of the phase transition would affect the background cosmology as well as perturbations. If the dark component of the Universe was relativistic at the time of big bang nucleosynthesis (BBN), it would contribute to radiation energy density and expansion rate of the Universe. Extra relativistic degrees of freedom,

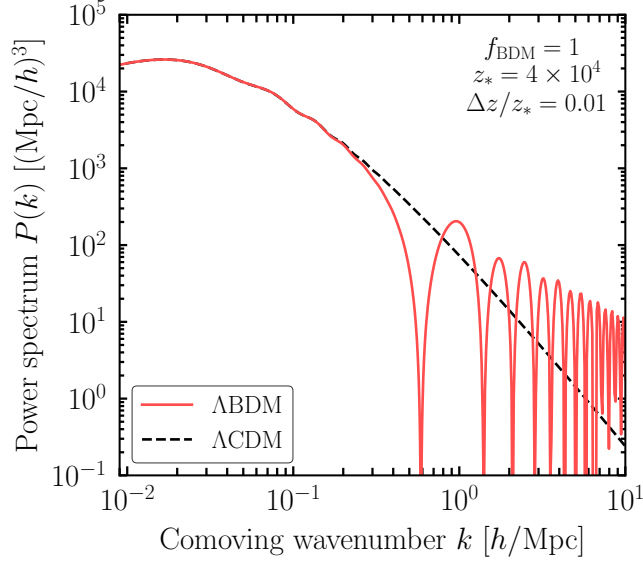


Figure 1. The matter power spectrum (solid red) as predicted in the Λ BDM cosmology with a fast phase transition at redshift $z_* = 4 \times 10^4$, and BDM comprises all of the dark matter. The Λ CDM power spectrum is also shown for comparison (dashed black).

parameterized by ΔN_{eff} (the extra neutrino degrees of freedom having same energy density), would modify the primordial nucleosynthesis if the phase transition takes place after the BBN epoch [22]. The cosmic microwave background (CMB) data suggest that during the epoch of recombination most of the matter must have been CDM-like [1] and restricts the phase transition to happen before the recombination epoch. We could do slightly better and require that the phase transition happens before the redshift of matter-radiation equality, z_{eq} , so that we do not change z_{eq} . The background cosmological parameters, like the relative matter and radiation densities and the Hubble parameter, would go to the Λ CDM values after the phase transition. The effect on the cosmological observables, the CMB and matter power spectrum [1, 23], would therefore appear dominantly through the modification of the dark matter perturbations for modes which entered the horizon before the phase transition. We will see the small scale modes, which entered the horizon before the Λ CDM matter-radiation equality, and which are well measured by CMB and galaxy surveys, would yield the strongest limits on the parameters of the phase transition.

The initial evolution of the matter perturbations after the phase transition is ballistic and results in interesting deviations in the perturbations compared to the CDM of the standard cosmological model. A sample of this behavior is shown in Fig. 1, for a phase transition at the redshift $z_* = 4 \times 10^4$ happening over a redshift-range $\Delta z = 0.01 z_*$ for BDM forming all of dark matter. We will also consider cosmologies where BDM forms only a fraction f_{BDM} of dark matter and the remaining $1 - f_{\text{BDM}}$ fraction is contributed by the standard CDM. As one can see, not only does the matter power spectrum exhibit acoustic oscillations at small scales, the power at the acoustic peaks exceeds the power in a standard Λ CDM model. The physics of BDM acoustic peaks is similar to that of baryon acoustic oscillations (BAOs) [24, 25]. We will see that, similar to the velocity overshoot effect in BAOs which results in phase shift in the BAO peaks w.r.t the acoustic peaks in the CMB, the origin of

the BDM acoustic peaks lies with the velocity perturbations at the time of phase transition and they correspond to the extrema of the velocity perturbations. Both the negative minima and the positive maxima of the BDM transfer function give rise to the peaks in the power spectrum. If not all of dark matter is BDM, the alternate BDM transfer function extrema would have either same or opposite sign to that of the CDM transfer function. The two DM components would alternately add constructively and destructively for successive extrema giving prominent asymmetry in the heights of odd vs even acoustic peaks in the total matter power spectrum. The features we see are similar to the charged massive particle model in Refs. [26, 27] also studied in Ref. [28] and have similar origin, namely, the initial velocity perturbations derived from a previous acoustic phase. These features are distinct from those of the other nonstandard models for which the growth of perturbations has been studied in detail [29–44]. The purpose of this paper is to introduce this BDM model, highlight its predictions, and explain them analytically. We will also discuss qualitative constraints on this model from existing CMB and galaxy surveys but leave a more detailed parameter space study for future work.

2 Ballistic Dark Matter: Model & Methods

We consider an effective macroscopic model for the dark sector, remaining agnostic to its detailed particle physics underpinnings. We assume that at early times the dark sector comprises of self-interacting relativistic species, that we call as the dark radiation (DR) phase, and it transitions to non-interacting non-relativistic particles, i.e., dark matter (DM) phase, at a redshift z_* with the corresponding scale factor denoted by a_* . We further assume that the anisotropic stress and all higher order moment perturbations in the Boltzmann hierarchy vanish, leaving only the density and velocity perturbations and allowing the DR phase to be described by its equation of state. This assumption can be relaxed, at the cost of working with the full stress-energy tensor [45]. In the cosmological context, such an evolution can be encoded in a time-varying equation of state (EoS) parameter for the BDM fluid,

$$w_B(z) = \begin{cases} 1/3 & z \gg z_* \text{ (before transition)} \\ 0 & z \ll z_* \text{ (after transition)}. \end{cases} \quad (2.1)$$

The subscript B will denote quantities associated to the BDM fluid.

Exactly how the EoS transitions between these two limits would depend on the details of the particle physics model of BDM. We expect that the cosmological observables, like the matter power spectrum, would be sensitive to the time or redshift of phase transition and how long the transition period lasts. Based on these considerations, we adopt the following simple model for the EoS during the phase transition,

$$w_B = \frac{1}{6} \left[1 - \tanh \left(\frac{a - a_*}{\Delta} \right) \right], \quad (2.2)$$

where Δ parametrizes the extent in scale factor over which the transition takes place. Note that as long as $\Delta \ll a_*$ and $a_* \ll 1$, we have $|\Delta/a_*| \approx |\Delta z/z_*|$, where Δz is the redshift-duration of phase transition. We will often refer to redshift instead of scale factor to give a more intuitive sense of when the transition takes place and how long it lasts.

In general, BDM may form only a fraction f_{BDM} of the total dark matter energy density. To parametrize this possibility, we define

$$f_{\text{BDM}} = \frac{\Omega_{\text{BDM}}}{\Omega_{\text{BDM}} + \Omega_{\text{CDM}}}, \quad (2.3)$$

as the present-day ratio of BDM to total dark matter, with the remaining fraction being CDM-like at all epochs.

We will also be interested in how perturbations grow in the presence of BDM. The equations for the linear perturbations of the BDM fluid in the *conformal Newtonian gauge* can be written as:

$$\dot{\delta}_B = -(1 + w_B)(\theta_B + 3\dot{\phi}) - 3\frac{\dot{a}}{a}(c_s^2 - w_B)\delta_B, \quad (2.4)$$

$$\dot{\theta}_B = -\frac{\dot{a}}{a}(1 - 3w_B)\theta_B - \frac{\dot{w}_B}{1 + w_B}\theta_B + \frac{c_s^2}{1 + w_B}k^2\delta_B + k^2\psi. \quad (2.5)$$

Here $\delta_B \equiv \delta\rho_B/\rho_B$ is the fractional density perturbation, $\theta_B \equiv ikv_B$ is the velocity perturbation divergence, and c_s is the speed of sound in the BDM fluid. The scalar metric perturbations are ϕ and ψ . We follow the sign convention of Ref. [46] for ϕ , which differs by a sign from Ref. [47]. All derivatives are w.r.t. the conformal time τ . The second term on the RHS of the first equation vanishes because we assume that the EoS does not depend on the energy density, and hence the speed of sound $c_s^2 \equiv \delta P/\delta\rho = w$. We can combine Eqs. (2.4) and (2.5) to get a second order equation for δ_B .

$$\begin{aligned} \ddot{\delta}_B + \frac{\dot{a}}{a}(1 - 3w_B)\dot{\delta}_B + k^2w_B\delta_B &= F, \\ F &\equiv -3\frac{\dot{a}}{a}(1 - 3w_B)(1 + w_B)\dot{\phi} - 3\dot{w}_B\dot{\phi} - 3(1 + w_B)\ddot{\phi} - (1 + w_B)k^2\psi. \end{aligned} \quad (2.6)$$

This is a damped forced oscillator equation for δ_B , with a forcing term F arising from metric perturbations which would be sourced by the self gravity of BDM as well as the other components of the Universe. Once the phase transition starts, the equation of state $w_B < 1/3$ and the damping term ($\propto \dot{\delta}_B$) becomes non-zero, damping the acoustic oscillations until the transition to DM phase is complete and the BDM fluid becomes non-interacting.

For the numerical results shown in this paper, we have implemented the BDM species, defined by Eqs. (2.2 - 2.5), in the public codes **CAMB** [48] and **CLASS** [49]. We then computed the transfer functions and the power spectra for this model using both codes and obtained essentially identical results. When using the synchronous gauge, we always keep a trace amount of ordinary CDM component to ensure that the gauge is well-defined. We will assume that the stress-energy tensor components remain continuous across the phase transition to connect the DR phase perturbations with the DM phase perturbations. We will also assume that no additional perturbations are created due to the phase transition.

3 Cosmological Signatures

3.1 Extra Relativistic Degrees of Freedom

The BDM before the phase transition acts like dark radiation and would contribute to the expansion of the Universe in the radiation dominated era modifying the expansion rate of the Universe. This effect can be quantified by effective relativistic degrees of freedom (in addition to photons), defined as

$$N_{\text{eff}} = \frac{\sum \rho_{\nu_i}}{\rho_{\nu}^{\text{FD}}} + \frac{\rho_{\text{DR}}}{\rho_{\nu}^{\text{FD}}} \quad (3.1)$$

$$\equiv N_{\text{eff}}^{\text{SM}} + \Delta N_{\text{eff}}. \quad (3.2)$$

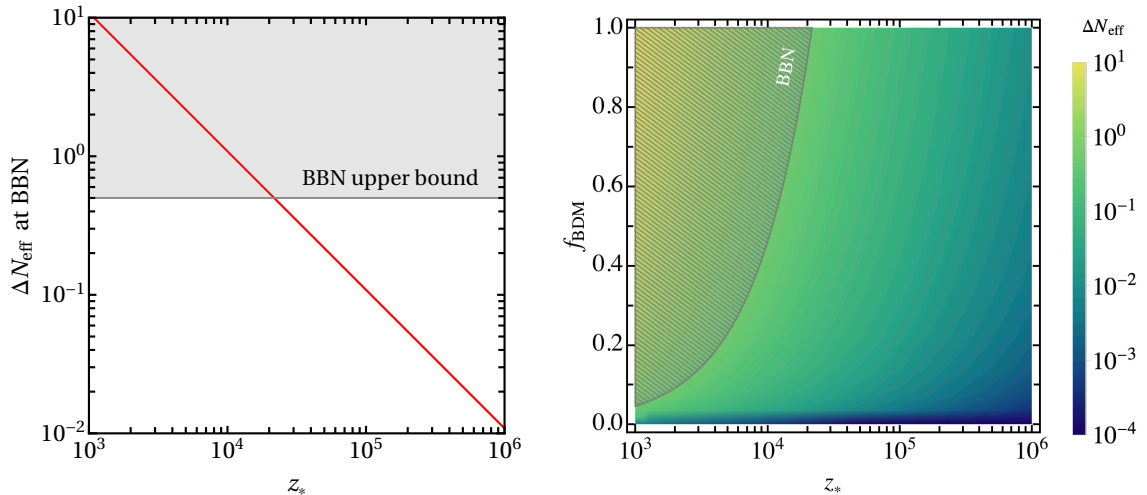


Figure 2. (Left) ΔN_{eff} at BBN for a BDM transition at z_* for $f_{\text{BDM}} = 1$. The upper bound is from primordial element abundance measurement that restricts $\Delta N_{\text{eff}} < 0.5$ [22, 55]. (Right) The gray-striped region in the $z_* - f_{\text{BDM}}$ plane is ruled out by the BBN constraint.

where ρ_{ν_i} is the energy density of i^{th} neutrino, ρ_{ν}^{FD} is the energy density of a single neutrino species assuming a thermal Fermi-Dirac distribution and no energy gain during the electron-positron annihilation epoch, and ρ_{DR} is the energy density of dark radiation. The theoretical prediction in standard Λ CDM cosmology with only standard model neutrinos contributing to N_{eff} is $N_{\text{eff}}^{\text{SM}} = 3.046$; the extra 0.046 taking into account the energy gained by neutrinos during the electron-positron annihilation [50–54]. We have defined ΔN_{eff} as the contribution by new physics.

The quantity ΔN_{eff} is constrained by both CMB and big bang nucleosynthesis (BBN) observation data. The CMB experiments, such as Planck, are sensitive to the amount of radiation present during recombination at $z \sim 1100$. The DR in our BDM model never thermalized with the visible sector. Also the time of phase transition must be much earlier than the recombination era and the era of matter radiation equality in order to satisfy the current cosmological constraints on the dark matter power spectrum. Therefore, the CMB anisotropy constraints on N_{eff} do not apply to our model because by the time of recombination BDM has the same background evolution as the CDM. Here we are implicitly assuming that all of the energy density in the BDM converts to dark matter. If this is not the case, and some energy remains as radiation, the constraint from CMB may also be important. However, if the phase transition happens after the BBN then DR in BDM model will certainly contribute to the N_{eff} at the time of BBN and can be constrained from the measurement of the primordial helium and deuterium abundance [22, 55]. The strongest BBN constraints at present are given by $N_{\text{eff}} = 3.28 \pm 0.28$ [55] or $\Delta N_{\text{eff}} \lesssim 0.5$.

In Fig. 2, we show the change in ΔN_{eff} at the time of BBN as a function of z_* . For $f_{\text{BDM}} = 1$, one finds $z_* \gtrsim 2 \times 10^4$. Note the $\simeq 1/z_*$ scaling of the limit. This is obvious because the energy density due to BDM is fixed by requiring that it reproduce the present-day dark matter energy density. The excess radiation in the BBN epoch thus simply scales with the relative factor $(1 + z_{\text{BBN}})/(1 + z_*)$. In the right panel of Fig. 2, the variation of ΔN_{eff} in the plane of $z_* - f_{\text{BDM}}$ is shown. The BBN constraint rules out the gray-striped

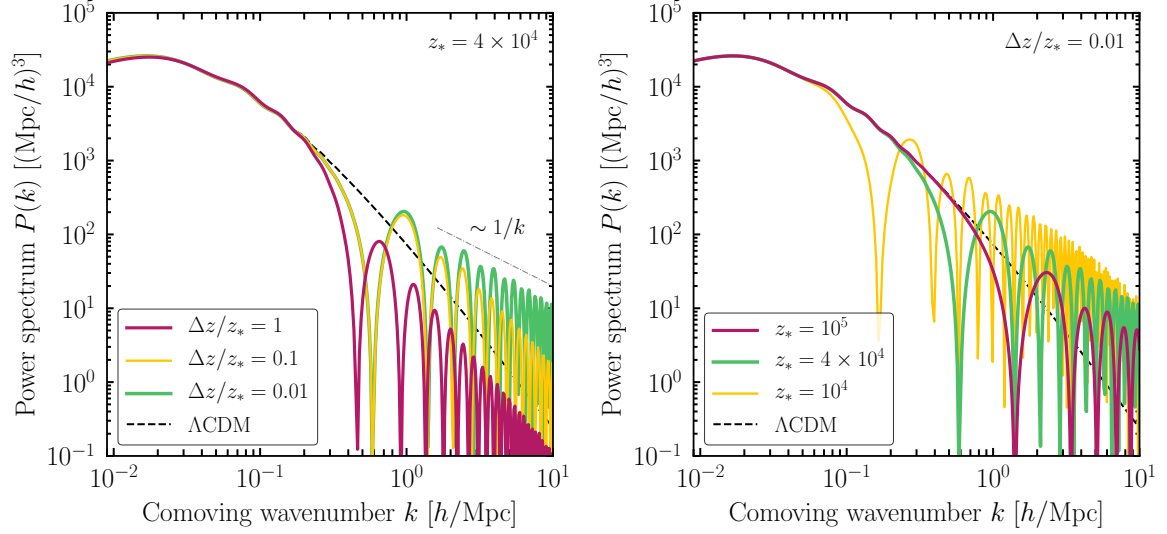


Figure 3. (Left) The matter power spectrum in a Λ BDM cosmology with phase transition at $z_* = 4 \times 10^4$, but with different transition widths $\Delta z/z_* = 1$ (purple), 0.1 (yellow), and 0.01 (green). (Right) The same matter power spectrum with different phase transition redshifts $z_* = 10^5$ (purple), 4×10^4 (green), and 10^4 (yellow), but now for a fixed width $\Delta z/z_* = 0.01$. For comparison, the Λ CDM power spectrum is shown as a dashed black curve in both panels. Note the enhancement of power at the acoustic peaks at small scales relative to the Λ CDM case.

region. However, we will see that the strongest effects of BDM would be on the matter power spectrum, and through it also on the CMB anisotropy spectrum, resulting in much stronger constraints than the BBN constraints on ΔN_{eff} . In other words, in the allowed parameter space for BDM, the extra contribution to the radiation energy density before the phase transition will not be of concern.

3.2 Matter Power Spectrum

The main signature of BDM is through its impact on the matter density perturbations. Unlike in Λ CDM cosmology, here the BDM can support waves until the phase transition occurs at z_* , leading to acoustic oscillations for k modes inside the horizon at z_* . We will also see that the nature of these acoustic oscillations in BDM is somewhat different from the acoustic damping seen in models where CDM is allowed to interact with a radiation like species.

In Fig. 3, we show the dark matter power spectrum $P(k)$ in a Λ BDM cosmology for different values of the additional parameters of the theory, namely, the width of the phase transition $\Delta z/z_*$ and transition epoch z_* . In the left panel, the green, yellow and purple curves represent the matter power spectra for transition widths $\Delta z/z_* = 0.01$, 0.1, and 1, respectively. An important observation here is the relative suppression of the spectrum for slower phase transitions. This feature can be attributed to the second term ($\propto \dot{\delta}_B$) on the LHS of Eq.(2.6). This term acts as a *friction* term in the oscillator equation and damps the fluctuations during the span of the phase transition. The effect of the phase transition epochs, $z_* = 10^4$, 4×10^4 , and 10^5 , on the matter power spectrum is shown in the right panel of Fig. 3. The value of z_* decides the scale or wavenumber k_* that was entering the horizon at the time of phase transition. All modes with $k < k_*$ are unaffected and the power spectrum

is indistinguishable from the Λ CDM case. The modes with $k > k_*$ entered the horizon before the phase transition and experienced acoustic oscillations leading to the new features in the power spectrum. Of course, as one would expect, if the phase transition occurs at very early times the scale of acoustic oscillations moves to larger k , converging to the Λ CDM model in the limit $z_* \rightarrow \infty$.

3.2.1 Analytical Understanding of the Acoustic Peaks

To understand the effect of the phase transition on the evolution of the perturbations in a simple way, we first assume an instantaneous transition at conformal time τ_* , corresponding to the redshift z_* . Also, in this section, we shall assume $z_* > z_{eq}$, i.e., the phase transition happens inside the radiation-dominated era. With this instantaneous phase transition approximation, the evolution equation for δ_B , Eq. (2.6), in each phase can be written as:

$$\ddot{\delta}_B + \frac{k^2}{3}\delta_B = -4\ddot{\phi} - \frac{4}{3}k^2\psi, \quad \text{DR phase}, \quad (3.3)$$

$$\ddot{\delta}_B + \frac{\dot{a}}{a}\dot{\delta}_B = -3\ddot{\phi} - 3\frac{\dot{a}}{a}\dot{\phi} - k^2\psi, \quad \text{DM phase}. \quad (3.4)$$

In this section, we shall be interested only in those modes which entered the horizon much before τ_* . We know that the metric perturbations decay to zero after a mode k enters the horizon during the radiation-domination era. Therefore, if we ignore the potential-dependent source terms on the RHS of Eqs. (3.3) and (3.4), the BDM perturbation equation Eq. (3.3) has an oscillatory solution

$$\delta_B(x < x_*) = A \cos x, \quad (3.5)$$

where we have defined the dimensionless quantity $x \equiv k\tau/\sqrt{3}$ for convenience. We kept only the cosine solution, as required by the adiabatic initial conditions at $\tau = 0$. This solution represents perturbation modes with acoustic oscillations of frequency $k/\sqrt{3}$. After the phase transition the evolution of BDM is described by Eq. (3.4), yielding logarithmic growth during radiation domination,

$$\delta_B(x > x_*) = B \ln x + C. \quad (3.6)$$

To fix the constants of integration, B and C , we should know the T^0_0 and T^0_i components of the BDM stress-energy tensor at the end of the phase transition or at the beginning of the DM phase. Because we are trying to study the cosmology in a model-independent way, we consider the simplest possible choice, i.e., both these components of T^μ_ν are continuous during the phase transition. This assumption yields

$$\begin{aligned} (\delta_B)_{\text{DR}} &= (\delta_B)_{\text{DM}}, \\ (\dot{\delta}_B)_{\text{DR}} &= (\dot{\delta}_B)_{\text{DM}} - \dot{\phi}. \end{aligned} \quad (3.7)$$

Since the potential ϕ decays after the mode enters the horizon, we finally have continuous δ_B and $\dot{\delta}_B$ across the phase transition happening $x = x_*$. Their values at x_* act as the initial conditions for the perturbations in the ensuing DM phase. Therefore, the solutions of Eq.(3.5) and (3.6) need to be matched at $x = x_*$ by equating δ_B and $\dot{\delta}_B$. The final DM phase solution is then given by

$$\delta_B(x > x_*) = A \cos x_* - Ax_* \sin x_* \ln \left(\frac{x}{x_*} \right). \quad (3.8)$$

The constant A is set by the initial conditions or initial curvature perturbation. Although the evolution is always logarithmic during radiation dominated era, depending on the value of $x_* = k\tau_*/\sqrt{3}$, two extreme cases are possible in the DM phase:

$$\delta_B(x) = (-1)^n A, \quad \text{if } x_* = n\pi, \quad (3.9)$$

$$\delta_B(x) = (-1)^{n+1} A x_* \ln\left(\frac{x}{x_*}\right), \quad \text{if } x_* = \left(n + \frac{1}{2}\right)\pi. \quad (3.10)$$

Here n is any integer. For the modes with k such that $x_* = n\pi$, the density fluctuation does not grow at all after the phase transition. Eventually these modes at even multiples of $\pi/2$ (or zeros of the sine) at the phase transition will carry less power and correspond to the minima in the power spectrum. On the contrary, if $x_* = (n + 1/2)\pi$, these modes at odd multiples of $\pi/2$ at the phase transition (extrema of the sine function) will have logarithmic growth with maximum slope. This large initial slope or prefactor is responsible for fast initial growth which may, for sharp phase transitions, overtake the Λ CDM perturbation giving acoustic peaks that overshoot the Λ CDM power for the same k modes.

Physically these two families of solutions are caused by the different *velocities* of the perturbation at τ_* . The modes which were crossing zero and had maximum velocity at x_* , i.e., $|\dot{\delta}_B(x_*)| = A$, will continue moving *ballistically* with the same bulk velocity in the collisionless DM phase, until the initial velocity is redshifted away. This inherited extra *bulk velocity kick* w.r.t what we expect from just gravitational infall in standard CDM, results in a faster logarithmic growth for these modes compared to all other modes. On the other hand, the modes having maximum displacement and zero velocity at x_* , i.e., $|\dot{\delta}_B(x_*)| = 0$, will not grow initially because the prefactor of the logarithmic term in Eq. (3.8) vanishes. All other modes which do not belong to these two extreme cases also have logarithmic growth but with relatively smaller slope. After $\tau = \tau_{\text{eq}}$ in the matter-dominated era, all modes grow as $\delta_B \sim a \sim \tau^2$. These different types of mode evolution will reflect themselves in the shape of the matter power spectrum. In particular it is the peculiar or bulk velocities of acoustic oscillations, and hence the sine mode, which get imprinted in the matter power spectrum, similar to the phase shift experienced by the baryon acoustic oscillations w.r.t. to the acoustic oscillations imprinted in the CMB [24, 25].

In the left panel of Fig. 4, we show the evolution of δ_B as a function of τ for the mode $k = 2h/\text{Mpc}$ for five different values of τ_* . This is simply the analytical solution shown in Eq. (3.8). The color-coding represents the absolute value of $\dot{\delta}_B$, hence the absolute value of θ_B . The transition epochs are chosen such that $x_* = 3.5\pi, 3.85\pi, 4\pi, 4.15\pi$ and 4.5π , respectively. Until the phase transition the evolution is identical, but depending on x_* the curves emanate from the phase transition point with different colours (i.e., velocities) which can be seen in the zoomed-in version of the gray region in the inset. As was argued in Eq. (3.10), the cases $x_* = 3.5\pi$ and 4.5π correspond to the extrema of the sine function (or the peculiar velocities at the phase transition) which show fast growth of the perturbations, resulting in excess power at the acoustic peaks seen in Fig. 3. The case with $x_* = 4\pi$ is the zero of the sine function and has zero velocity but maximum density perturbation at $\tau = \tau_*$ and remains frozen at this value, lagging behind all other modes at late times. They correspond to the dips in the oscillatory part of the power spectrum. Other cases of $x_* = 3.85\pi$ and 4.15π have intermediate velocities at τ_* . Note how all peculiar velocities redshift as $\sim 1/a$ after the phase transition. Eventually, of course, the peculiar velocities sourced by gravitational potentials will take over.

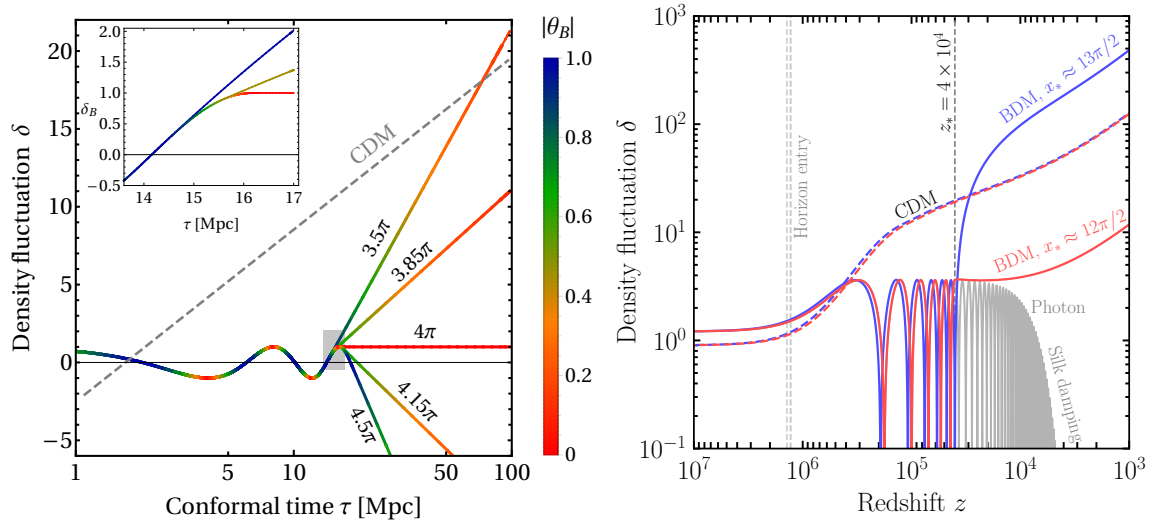


Figure 4. (Left) Analytical solution of the BDM linear perturbation equations for the mode $k = 2h/\text{Mpc}$. Five curves are shown with different τ_* s corresponding to $x_* = 3.5\pi, 3.85\pi, 4\pi, 4.15\pi$ and 4.5π , respectively. The colour of the curves represent the absolute value of the velocity perturbation $|\theta_B|$. A zoomed-in version of the gray region is shown in the inset. The dashed, gray line shows the evolution of the same mode in CDM perturbation. (Right) Numerical solution for evolution of two modes of BDM perturbation δ_B corresponding to a maximum ($x_* \approx 13\pi/2$) and a minimum ($x_* \approx 12\pi/2$) in the matter power spectrum. Corresponding CDM mode evolutions in ΛCDM cosmology are also shown as dashed curves. The other parameter values are $z_* = 4 \times 10^4$, $\Delta z/z_* = 10^{-2}$ and $f_{\text{BDM}} = 1$.

In the right panel of Fig. 4, we see that the numerical results show the same behavior as above. The two modes, $k = 4.305h/\text{Mpc}$ and $4.661h/\text{Mpc}$, roughly correspond to $x_* \simeq 12\pi/2$ and $13\pi/2$, respectively, for a phase transition at $z_* = 4 \times 10^4$. These modes lead to a dip and a peak, respectively, in the matter power spectrum. The perturbations remain constant at their initial values until the time of their respective horizon entry which happens when $k\tau \simeq 1$. Afterwards they start oscillating with a frequency $k/\sqrt{3}$. They continue to oscillate until τ_* , thereafter they start growing as $\sim \ln \tau$ during the radiation-domination era and as $\sim \tau^2$ in the matter-domination era. The same modes for δ_c in a ΛCDM cosmology are also shown in the dashed curves. As discussed in the preceding paragraph, the modes starting with extra *bulk velocity kicks* from the pre-phase transition oscillations overshoot the ΛCDM value and eventually acquire more power. They give rise to the peaks in Fig. 3. Whereas those perturbations which were at their maximum values at the time of phase transition (hence, zero velocity) grow at a much slower rate and lead to the dips in Fig. 3. Indeed the mode labeled by $x_* \approx 13\pi/2$ (solid blue, peak of the sine function), grows faster and goes above the ΛCDM curve (dashed blue, zero of the sine function), while the mode labeled by $x_* \approx 12\pi/2$ (red curve) remains below it. This gives rise to the oscillatory feature in the matter power spectrum in Fig. 1, with the upper envelop of the oscillations going above the ΛCDM expectation.

From Eq.(3.10), we note that the absolute value of maximum perturbation is proportional to the wavenumber k . Hence the transfer function $T(k)_{\text{max}} \sim k$. As a result, we expect

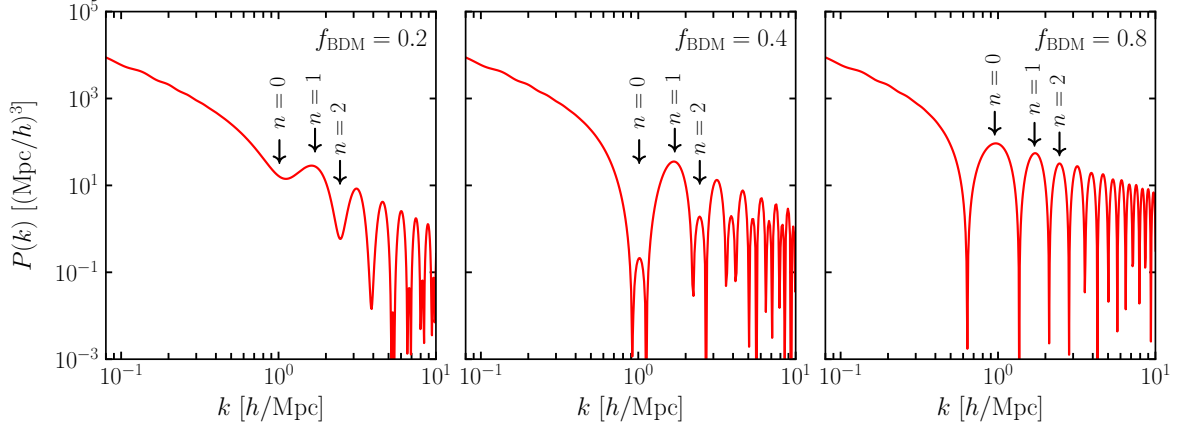


Figure 5. The matter power spectra for three different BDM fractions $f_{\text{BDM}} = 0.2, 0.4$ and 0.8 . The first three ‘peaks’ numbered by $n = 0, 1, 2$ (see Eq. (3.10) for details) are marked with black arrows.

the envelop of the peaks of the $P(k)$ to scale as $\sim 1/k$,

$$P(k)_{\text{max}} \equiv \frac{2\pi^2 \mathcal{P}_p}{k^3} T(k)_{\text{max}}^2 \sim 1/k, \quad (3.11)$$

where \mathcal{P}_p is the primordial scalar power spectrum defined as

$$\mathcal{P}_p = A_s \left(\frac{k}{k_0} \right)^{n_s - 1}, \quad (3.12)$$

in terms of the amplitude A_s , the scalar index $n_s = 0.96$, and the pivot scale k_0 [1]. The $1/k$ upper envelop of $P(k)$ predicted by Eq.(3.11) is evident in Fig.3 for the case of fast transition, $\Delta z/z_* = 0.01$, as shown by the dashed gray line.

3.2.2 Odd-Even Peak Asymmetry

An interesting asymmetry in the heights of the power spectrum peaks becomes apparent if the fraction of BDM is neither 0 nor 1. Three representative cases are shown in Fig.5 with $f_{\text{BDM}} = 0.2, 0.4$ and 0.8 , respectively. We have numbered the peaks according of value of n in Eq. (3.10) with the first peak given by $n = 0$ corresponding to first zero crossing of cosine (density) or first extrema of sine (peculiar velocity). First, we concentrate on the $f_{\text{BDM}} = 0.4$ case and observe that the heights of the odd-numbered peaks are greater than the even-numbered ones. To understand the reason behind this asymmetry, we plot in the left panel of Fig.6 the individual BDM and CDM transfer functions T_{B} (dashed orange) and T_{C} (dashed light blue), along with the total dark matter transfer function $T_{\text{DM}}(k)$ (solid black), which is defined as

$$T_{\text{DM}}(k) = f_{\text{BDM}} T_{\text{B}}(k) + (1 - f_{\text{BDM}}) T_{\text{C}}(k), \quad (3.13)$$

at a redshift $z = 3000$. Oscillations with amplitude growing with k are present in the BDM transfer function, $T_{\text{B}}(k)$, as expected. However, we now see that such oscillations, albeit with smaller amplitude, are also imprinted in the CDM transfer function T_{C} . This is the result of the CDM responding to the gravity of BDM or the gravitational potential ϕ which

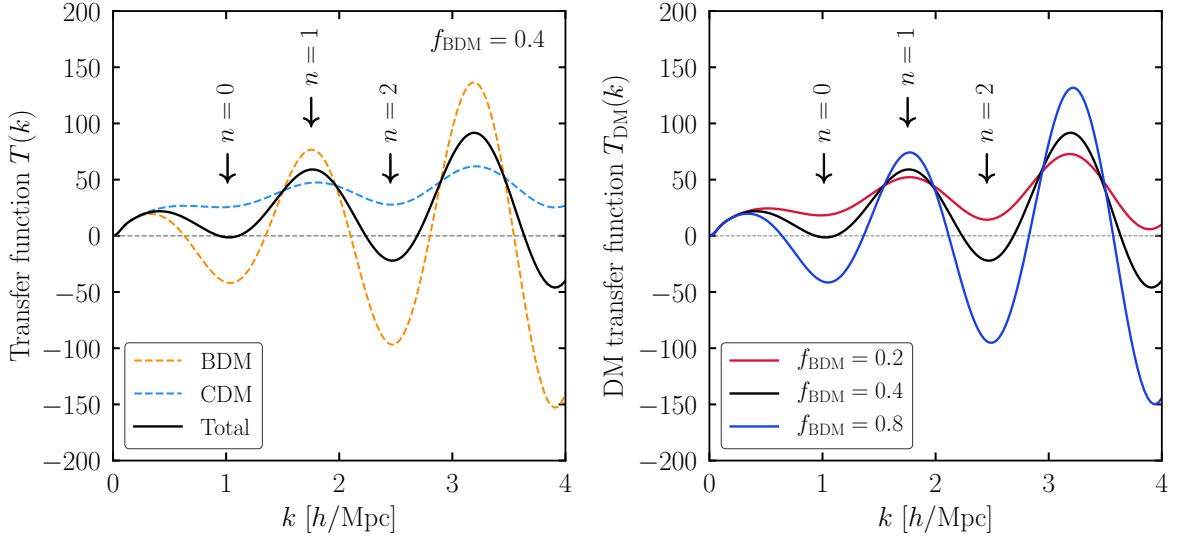


Figure 6. (Left) Individual transfer functions of BDM $T_B(k)$ (dashed orange), CDM $T_C(k)$ (dashed light blue), and the total dark matter transfer function $T_{DM} = f_{BDM}T_B + (1 - f_{BDM})T_C$ (solid black) at redshift $z = 3000$ for $f_{BDM} = 0.4$. (Right) Comparison between dark matter transfer functions $T_{DM}(k)$ computed for three different fractions of BDM, viz., $f_{BDM} = 0.2$ (red), 0.4 (blue), and 0.8 (green). Other phase transition parameters are $z_* = 4 \times 10^4$, $\Delta z/z_* = 10^{-2}$.

has contribution from T_B . Further, we observe the relative sign between the two transfer functions. At the positions of the peaks of T_B , the two transfer functions have the same sign and reinforce each other resulting in a larger magnitude of T_{DM} . On the other hand, at the troughs of T_B they have opposite signs and can partially cancel each other. These shallower troughs of the T_B , that are below zero, appear as smaller peaks in the matter power spectrum. This leads to the asymmetry between the consecutive maxima in the matter power spectrum in Fig. 5. Physically, the initial velocities of BDM at the phase transition for k modes corresponding to even values of n were such that the (BDM) matter flowed from out of the initial overdensities, which were the same for CDM and BDM according to the adiabatic initial conditions, and flowed into the initial underdensities and thus reducing the amplitude of perturbations for those modes. For the modes corresponding to odd values of n , the BDM matter flowed into the CDM overdensities and out of the CDM underdensities, increasing the density contrast.

Both components of the dark matter are needed in sizeable amount for the odd-even acoustic peak asymmetry to be prominent. This is evident from the $f_{BDM} = 0.2$ and 0.8 plots in Fig. 5 and the right panel of Fig. 6. For $f_{BDM} = 0.2$, the BDM has a sub-dominant contribution to the total power spectrum and the out of phase extrema of BDM (even- n) only result in giving minima in the total power spectrum. Thus only the odd- n modes result in acoustic peaks in the total matter power spectrum. As we increase f_{BDM} , the minima in the total transfer function become deeper and deeper and at some point cross zero (see Fig. 6, right panel). Once the total transfer function has a zero crossing, the zero-crossings become the deep minima in the matter power spectrum and the minima of the transfer function appear as additional peaks, doubling the number of acoustic peaks in the total power spectrum.

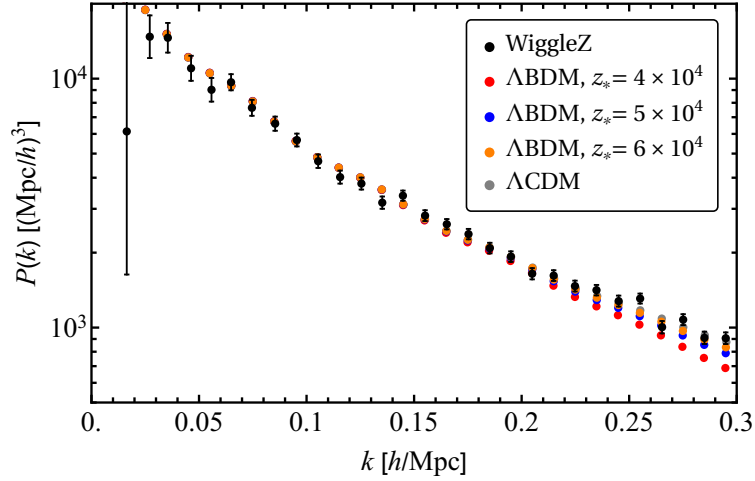


Figure 7. Comparison between the observed matter power spectrum by WiggleZ [3] and the theoretical power spectra for different transition redshifts, $z_* = 4 \times 10^4$, 5×10^4 , 6×10^4 .

The asymmetry, i.e., the relative heights of the consecutive maxima in the power spectrum is fixed once the initial peculiar velocities have redshifted away. Subsequently, the BDM and CDM can be treated as a single collisionless cold fluid, with a modified power spectrum which grows linearly with redshift identically to the CDM fluid in the standard Λ CDM cosmology. In particular, subsequent linear growth does not change the shape of the power spectrum and the asymmetry and acoustic features persist until today in linear theory.

3.3 Qualitative Constraints from the Matter and CMB Power Spectrum

As we have already discussed, the effective relativistic degrees of freedom during BBN already gives interesting constraints on the redshift of phase transition. A more stringent lower bound on z_* is given by the measurement of the dark matter power spectrum. From Fig. 3 we see that even a value $z_* = 10^4$ predicts a sharp drop in power at $k = 0.1h/\text{Mpc}$ near the second BAO peak. These scales are well measured at many redshifts by the current galaxy surveys like SDSS [23] and WiggleZ [3] and therefore $z_* = 10^4$ is clearly ruled out by the current matter power spectrum measurements. We show the WiggleZ data from the redshift range $0.5 < z < 0.7$ and theoretical Λ BDM power spectrum using the flat Λ CDM best-fit model parameters in the Table VII of Ref. [3] in Fig. 7 for different z_* . We have used the same binning as the WiggleZ data for the theoretical power spectrum and convolved it with the WiggleZ window function. As we can see, even when restricting to approximately linear modes, $k < 0.3h/\text{Mpc}$, we can already rule out z_* smaller than $\sim 5 \times 10^4$ by eye. We remind that this is a crude estimate, and to be more accurate one needs to do a more detailed study with degeneracies with other Λ CDM parameters, such as n_s , taken into account.

We will also expect modifications to the CMB anisotropy power spectrum at small angular scales as it is sensitive to the total dark matter power spectrum at the time of recombination. In a flat Universe, the mode k_* corresponds to an approximate angular scale of $\ell_* \simeq k_* \tau_0$ where $\tau_0 = 1.4 \times 10^4 \text{ Mpc}$ is the conformal time today. Therefore the observability of this effect in the CMB angular power spectrum would depend on the value of k_* . The smallest scale probed by the current Planck experiment corresponds to $\ell_{max} = 2500$ implying

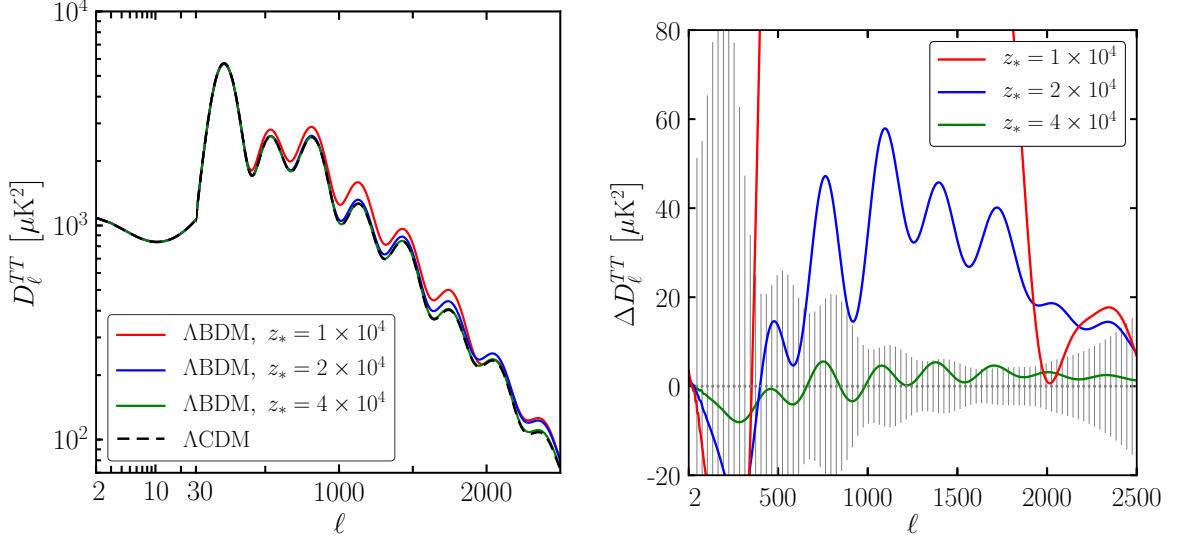


Figure 8. (Left) Effects in the CMB TT power spectrum is shown for $z_* = 10^4$ (red), 2×10^4 (blue), and 4×10^4 (green) with $\Delta z/z_* = 0.01$ and $f_{\text{BDM}} = 1$. (Right) The difference between ΛBDM and ΛCDM powers $\Delta D_\ell^{TT} \equiv (D_\ell^{TT})_{\Lambda\text{BDM}} - (D_\ell^{TT})_{\Lambda\text{CDM}}$. We compare this ΔD_ℓ^{TT} with the Planck high- ℓ ($47 \leq \ell \leq 2499$) binned data, and conclude that the Planck data puts a rough lower limit on the transition redshift $z_* \gtrsim 4 \times 10^4$.

a value of $k_* \simeq 0.2h/\text{Mpc}$, therefore a sensitivity to $z_* \lesssim 6 \times 10^4$. The typical changes expected in the CMB TT angular power spectrum are shown in the left panel of Fig. 8 for $z_* = 10^4$ (red), 2×10^4 (blue) and 4×10^4 (green). We use the best-fit values of ΛCDM parameters from the Planck experiment [1]. In the right panel of Fig. 8, we plot the difference between ΛBDM and ΛCDM powers $\Delta D_\ell^{TT} \equiv (D_\ell^{TT})_{\Lambda\text{BDM}} - (D_\ell^{TT})_{\Lambda\text{CDM}}$ together with the Planck high- ℓ ($47 \leq \ell \leq 2499$) binned data error bars. We conclude that values of transition redshift $z_* \lesssim 4 \times 10^4$ are not consistent with the CMB data. The next-generation CMB observation experiments promise to probe even smaller angular scales and correspondingly smaller k values [56].

The matter power spectrum and the CMB power spectrum at present would give comparable constraints on the BDM parameters (z_* , $\Delta z/z_*$, f_{BDM}) with the constraints from the matter power spectrum expected to be stronger. We leave a more detailed Markov Chain Monte Carlo study of the ΛBDM parameters using current CMB temperature and polarization data and matter power spectrum for a future publication.

4 Summary & Conclusions

We have studied the cosmological consequences of a class of dark matter models defined by two main properties:

1. The time when the dark matter becomes non-relativistic coincides with it also becoming collisionless and the dark fluid is strongly interacting before this phase transition.
2. This phase transition happens much later than the decoupling of dark matter from the visible sector and in particular happens after BBN and before recombination.

Before the phase transition to non-relativistic collisionless dark matter, the radiation-like particles were tightly coupled together and constituted a perfect fluid. The pressure in the fluid supports acoustic oscillations and stalls the growth of density perturbations during the period between a mode's horizon entry and the phase transition at τ_* . The consequence of the above two features is that the non-relativistic phase of the dark matter starts with a non-zero peculiar velocities which are a sinusoidally oscillating function of the mode k , and which are 90 degrees out of phase w.r.t. the density fluctuations, inherited from the previous tightly coupled relativistic phase. The initial evolution in the collisionless phase is ballistic until the initial acoustic peculiar velocities have been redshifted away, hence the name Ballistic Dark Matter or BDM. Afterwards the perturbations grow in a similar fashion as in the Λ CDM cosmology. The initial evolution after the phase transition of a mode is therefore driven almost entirely by the peculiar velocities at the phase transition. The modes which had the maximum velocity at τ_* grow fastest and the modes for which the density perturbation was at the maximum amplitude and hence had zero velocity have the slowest initial growth. The acoustic oscillations before the phase transition are thus imprinted on the dark matter power spectrum. For fast phase transitions, the acoustic peaks in the matter power spectrum, driven by high initial peculiar velocities, can exceed the Λ CDM power. The excess growth of power relative to the Λ CDM case can be suppressed if the phase transition happens rather slowly. A gradual variation of the EoS of the dark sector fluid leads to damping of perturbations.

If BDM does not dominate the matter energy density in the Universe then an asymmetry arises in the peak heights of the matter power spectrum. This happens because the transfer functions of CDM and BDM can be in-phase or out-of phase at the extrema of the BDM transfer function. The minima and maxima of the BDM transfer function have opposite sign and would give rise to similar amplitude acoustic peaks if BDM formed all of dark matter. The CDM transfer function on the other hand does not change sign as a function of k . Therefore successive extrema of the BDM would have alternatively the same and the opposite sign to that of CDM and the two can add constructively or destructively. The acoustic peaks in the total matter power spectrum would be therefore alternate between enhancement and suppression giving an odd-even peak asymmetry.

By varying the three parameters of our BDM model, the redshift of phase transition, z_* , the duration of phase transition, $\Delta z/z_*$, and the fraction of dark matter formed by BDM, f_{BDM} , we can get a rich variety of features and, in particular, tune the matter power spectrum to be enhanced or suppressed at particular wavenumbers k . We have shown, by comparison with existing data, that for fast transitions and all of DM formed by BDM, the phase transitions must happen at $z_* > 5 \times 10^4$. Our results indicate that Ballistic Dark Matter has rich cosmological phenomenology and motivate a more detailed study of the consequences of such a dark matter model on the large scale structure, in particular in the non-linear regime, in the future.

Acknowledgments

We gratefully acknowledge useful discussions with Subhajit Ghosh, Sourendu Gupta, and Nilmani Mathur. BD was partially supported through a Ramanujan Fellowship of the Dept. of Science and Technology, Government of India and the Max-Planck-Gesellschaft funded Max Planck Partner Group between Max Planck Institute for Physics, Munich and Tata Institute of Fundamental Research. RK was supported by Science and Engineering Research Board (SERB) of Department of Science and Technology, Govt. of India through SERB

grant ECR/2015/000078 and Max Planck Partner Group between Max Planck Institute for Astrophysics, Garching and Tata Institute of Fundamental Research.

References

- [1] **Planck** Collaboration, P. A. R. Ade et al., *Planck 2015 results. XIII. Cosmological parameters*, *Astron. Astrophys.* **594** (2016) A13, [[arXiv:1502.01589](#)].
- [2] M. Costanzi et al., *Dark Energy Survey Year 1 Results: Methods for Cluster Cosmology and Application to the SDSS*, [arXiv:1810.09456](#).
- [3] D. Parkinson, S. Riemer-Sørensen, C. Blake, G. B. Poole, T. M. Davis, S. Brough, M. Colless, C. Contreras, W. Couch, S. Croom, D. Croton, M. J. Drinkwater, K. Forster, D. Gilbank, M. Gladders, K. Glazebrook, B. Jelliffe, R. J. Jurek, I.-h. Li, B. Madore, D. C. Martin, K. Pimbblet, M. Pracy, R. Sharp, E. Wisnioski, D. Woods, T. K. Wyder, and H. K. C. Yee, *The WiggleZ Dark Energy Survey: Final data release and cosmological results*, *Phys. Rev. D* **86** (Nov., 2012) 103518, [[arXiv:1210.2130](#)].
- [4] **SDSS** Collaboration, M. Tegmark et al., *Cosmological Constraints from the SDSS Luminous Red Galaxies*, *Phys. Rev.* **D74** (2006) 123507, [[astro-ph/0608632](#)].
- [5] **SDSS** Collaboration, M. Tegmark et al., *Cosmological parameters from SDSS and WMAP*, *Phys. Rev.* **D69** (2004) 103501, [[astro-ph/0310723](#)].
- [6] D. Clowe, M. Bradac, A. H. Gonzalez, M. Markevitch, S. W. Randall, C. Jones, and D. Zaritsky, *A direct empirical proof of the existence of dark matter*, *Astrophys. J.* **648** (2006) L109–L113, [[astro-ph/0608407](#)].
- [7] K. G. Begeman, A. H. Broeils, and R. H. Sanders, *Extended rotation curves of spiral galaxies: Dark haloes and modified dynamics*, *Mon. Not. Roy. Astron. Soc.* **249** (1991) 523.
- [8] S. Heeba, F. Kahlhoefer, and P. Stcker, *Freeze-in production of decaying dark matter in five steps*, [arXiv:1809.04849](#).
- [9] G. Steigman, B. Dasgupta, and J. F. Beacom, *Precise Relic WIMP Abundance and its Impact on Searches for Dark Matter Annihilation*, *Phys. Rev.* **D86** (2012) 023506, [[arXiv:1204.3622](#)].
- [10] E. D. Carlson, M. E. Machacek, and L. J. Hall, *Self-interacting dark matter*, *Astrophys. J.* **398** (1992) 43–52.
- [11] L. B. Okun, *THETONS*, *JETP Lett.* **31** (1980) 144–147. [*Pisma Zh. Eksp. Teor. Fiz.* 31,156(1979)].
- [12] A. E. Faraggi and M. Pospelov, *Selfinteracting dark matter from the hidden heterotic string sector*, *Astropart. Phys.* **16** (2002) 451–461, [[hep-ph/0008223](#)].
- [13] J. E. Juknevich, D. Melnikov, and M. J. Strassler, *A Pure-Glue Hidden Valley I. States and Decays*, *JHEP* **07** (2009) 055, [[arXiv:0903.0883](#)].
- [14] B. S. Acharya, M. Fairbairn, and E. Hardy, *Glueball dark matter in non-standard cosmologies*, *JHEP* **07** (2017) 100, [[arXiv:1704.01804](#)].
- [15] S. Nussinov, *Technocosmology could a technibaryon excess provide a natural missing mass candidate?*, *Physics Letters B* **165** (1985), no. 1 55 – 58.
- [16] S. Barr, R. S. Chivukula, and E. Farhi, *Electroweak fermion number violation and the production of stable particles in the early universe*, *Physics Letters B* **241** (1990), no. 3 387 – 391.
- [17] S. M. Barr, *Baryogenesis, sphalerons and the cogeneration of dark matter*, *Phys. Rev.* **D44** (1991) 3062–3066.

- [18] D. B. Kaplan, *Single explanation for both baryon and dark matter densities*, *Phys. Rev. Lett.* **68** (Feb, 1992) 741–743.
- [19] D. E. Kaplan, M. A. Luty, and K. M. Zurek, *Asymmetric Dark Matter*, *Phys. Rev.* **D79** (2009) 115016, [[arXiv:0901.4117](#)].
- [20] G. D. Kribs, T. S. Roy, J. Terning, and K. M. Zurek, *Quirky Composite Dark Matter*, *Phys. Rev.* **D81** (2010) 095001, [[arXiv:0909.2034](#)].
- [21] M. Blennow, B. Dasgupta, E. Fernandez-Martinez, and N. Rius, *Aidnogenesis via Leptogenesis and Dark Sphalerons*, *JHEP* **03** (2011) 014, [[arXiv:1009.3159](#)].
- [22] G. Mangano and P. D. Serpico, *A robust upper limit on N from BBN, circa 2011*, *Physics Letters B* **701** (July, 2011) 296–299, [[arXiv:1103.1261](#)].
- [23] W. J. Percival et al., *The shape of the SDSS DR5 galaxy power spectrum*, *Astrophys. J.* **657** (2007) 645–663, [[astro-ph/0608636](#)].
- [24] R. A. Sunyaev and Y. B. Zeldovich, *Small-Scale Fluctuations of Relic Radiation*, *Astrophysics and Space Science* **7** (Apr., 1970) 3–19.
- [25] D. J. Eisenstein and W. Hu, *Baryonic Features in the Matter Transfer Function*, *ApJ* **496** (Mar., 1998) 605–614, [[astro-ph/9709112](#)].
- [26] A. Kamada, K. Kohri, T. Takahashi, and N. Yoshida, *Effects of electrically charged dark matter on cosmic microwave background anisotropies*, *Phys. Rev.* **D95** (2017), no. 2 023502, [[arXiv:1604.07926](#)].
- [27] A. Kamada and T. Takahashi, *Dark matter kinetic decoupling with a light particle*, *JCAP* **1801** (2018), no. 01 047, [[arXiv:1703.02338](#)].
- [28] A. Sarkar, S. K. Sethi, and S. Das, *The effects of the small-scale behaviour of dark matter power spectrum on CMB spectral distortion*, *JCAP* **1707** (2017), no. 07 012, [[arXiv:1701.07273](#)].
- [29] C. Boehm, P. Fayet, and R. Schaeffer, *Constraining dark matter candidates from structure formation*, *Phys. Lett.* **B518** (2001) 8–14, [[astro-ph/0012504](#)].
- [30] C. Boehm, A. Riazuelo, S. H. Hansen, and R. Schaeffer, *Interacting dark matter disguised as warm dark matter*, *Phys. Rev.* **D66** (2002) 083505, [[astro-ph/0112522](#)].
- [31] X.-l. Chen, S. Hannestad, and R. J. Scherrer, *Cosmic microwave background and large scale structure limits on the interaction between dark matter and baryons*, *Phys. Rev.* **D65** (2002) 123515, [[astro-ph/0202496](#)].
- [32] K. Sigurdson and M. Kamionkowski, *Charged - particle decay and suppression of small - scale power*, *Phys. Rev. Lett.* **92** (2004) 171302, [[astro-ph/0311486](#)].
- [33] A. Nusser, S. S. Gubser, and P. J. E. Peebles, *Structure formation with a long-range scalar dark matter interaction*, *Phys. Rev.* **D71** (2005) 083505, [[astro-ph/0412586](#)].
- [34] S. Das and N. Weiner, *Late Forming Dark Matter in Theories of Neutrino Dark Energy*, *Phys. Rev.* **D84** (2011) 123511, [[astro-ph/0611353](#)].
- [35] L. G. van den Aarssen, T. Bringmann, and C. Pfrommer, *Is dark matter with long-range interactions a solution to all small-scale problems of Λ CDM cosmology?*, *Phys. Rev. Lett.* **109** (2012) 231301, [[arXiv:1205.5809](#)].
- [36] R. J. Wilkinson, J. Lesgourgues, and C. Boehm, *Using the CMB angular power spectrum to study Dark Matter-photon interactions*, *JCAP* **1404** (2014) 026, [[arXiv:1309.7588](#)].
- [37] R. J. Wilkinson, C. Boehm, and J. Lesgourgues, *Constraining Dark Matter-Neutrino Interactions using the CMB and Large-Scale Structure*, *JCAP* **1405** (2014) 011, [[arXiv:1401.7597](#)].

- [38] X. Chu and B. Dasgupta, *Dark Radiation Alleviates Problems with Dark Matter Halos*, *Phys. Rev. Lett.* **113** (2014), no. 16 161301, [[arXiv:1404.6127](#)].
- [39] M. R. Buckley, J. Zavala, F.-Y. Cyr-Racine, K. Sigurdson, and M. Vogelsberger, *Scattering, Damping, and Acoustic Oscillations: Simulating the Structure of Dark Matter Halos with Relativistic Force Carriers*, *Phys. Rev.* **D90** (2014), no. 4 043524, [[arXiv:1405.2075](#)].
- [40] M. Archidiacono, S. Hannestad, R. S. Hansen, and T. Tram, *Sterile neutrinos with pseudoscalar self-interactions and cosmology*, *Phys. Rev.* **D93** (2016), no. 4 045004, [[arXiv:1508.02504](#)].
- [41] F.-Y. Cyr-Racine, K. Sigurdson, J. Zavala, T. Bringmann, M. Vogelsberger, and C. Pfrommer, *ETHOSan effective theory of structure formation: From dark particle physics to the matter distribution of the Universe*, *Phys. Rev.* **D93** (2016), no. 12 123527, [[arXiv:1512.05344](#)].
- [42] Z. Chacko, Y. Cui, S. Hong, T. Okui, and Y. Tsai, *Partially Acoustic Dark Matter, Interacting Dark Radiation, and Large Scale Structure*, *JHEP* **12** (2016) 108, [[arXiv:1609.03569](#)].
- [43] J. A. Dror, E. Kuflik, B. Melcher, and S. Watson, *Concentrated dark matter: Enhanced small-scale structure from decaying dark matter*, *Phys. Rev.* **D97** (2018), no. 6 063524, [[arXiv:1711.04773](#)].
- [44] M. A. Buen-Abad, R. Emami, and M. Schmaltz, *Cannibal Dark Matter and Large Scale Structure*, [arXiv:1803.08062](#).
- [45] W. Hu, *Structure formation with generalized dark matter*, *Astrophys. J.* **506** (1998) 485–494, [[astro-ph/9801234](#)].
- [46] S. Dodelson, *Modern Cosmology*. Academic Press, Amsterdam, 2003.
- [47] C.-P. Ma and E. Bertschinger, *Cosmological perturbation theory in the synchronous and conformal Newtonian gauges*, *Astrophys. J.* **455** (1995) 7–25, [[astro-ph/9506072](#)].
- [48] A. Lewis, A. Challinor, and A. Lasenby, *Efficient computation of CMB anisotropies in closed FRW models*, *Astrophys. J.* **538** (2000) 473–476, [[astro-ph/9911177](#)].
- [49] D. Blas, J. Lesgourgues, and T. Tram, *The Cosmic Linear Anisotropy Solving System (CLASS). Part II: Approximation schemes*, *JCAP* **7** (July, 2011) 034, [[arXiv:1104.2933](#)].
- [50] A. D. Dolgov and M. Fukugita, *Nonequilibrium effect of the neutrino distribution on primordial helium synthesis*, *Phys.Rev.D* **46** (Dec., 1992) 5378–5382.
- [51] S. Hannestad and J. Madsen, *Neutrino decoupling in the early Universe*, *Phys.Rev.D* **52** (Aug., 1995) 1764–1769, [[astro-ph/9506015](#)].
- [52] A. D. Dolgov, S. H. Hansen, and D. V. Semikoz, *Non-equilibrium corrections to the spectra of massless neutrinos in the early universe*, *Nuclear Physics B* **503** (Feb., 1997) 426–444, [[hep-ph/9703315](#)].
- [53] N. Fornengo, C. W. Kim, and J. Song, *Finite temperature effects on the neutrino decoupling in the early Universe*, *Phys.Rev.D* **56** (Oct., 1997) 5123–5134, [[hep-ph/9702324](#)].
- [54] G. Mangano, G. Miele, S. Pastor, and M. Peloso, *A precision calculation of the effective number of cosmological neutrinos*, *Physics Letters B* **534** (May, 2002) 8–16, [[astro-ph/0111408](#)].
- [55] R. Cooke, M. Pettini, R. A. Jorgenson, M. T. Murphy, and C. C. Steidel, *Precision measures of the primordial abundance of deuterium*, *Astrophys. J.* **781** (2014), no. 1 31, [[arXiv:1308.3240](#)].
- [56] **CMB-S4** Collaboration, K. N. Abazajian et al., *CMB-S4 Science Book, First Edition*, [arXiv:1610.02743](#).